Improved Smith predictor control for fast steering mirror system

Zheng Cao[1, 2, 3], Jing Chen[1, 2, 3], Chao Deng[1, 2, 3], Yao Mao[1, 2] and Zhijun Li[1, 2]

[1]Key Laboratory of Optical Engineering, Chinese Academy of Sciences, Chengdu, China, 610209
[2]Institute of Optics and Electronics, Chinese Academy of Science, Chengdu, China, 610209
[3]University of Chinese Academy of Sciences, Beijing, China, 100039

Abstract. In this paper, a novel Smith predictor control strategy improved by a high bandwidth inner loop for fast steering mirror (FSM) tracking control system based on a charge-coupled device (CCD) and rate sensor is proposed. A high bandwidth velocity closed-loop constructed by a fiber-optic gyroscope is utilized to provide a robust controlled plant for the Smith predictor controller. Usually, due to the mechanical resonances and time delay induced by a low CCD sampling rate, the tracking performance of FSM system is insufficient when suffering uncertain input command. Therefore, the Smith predictor control, which is famous for its delay-free characteristic and suitable for regulating systems with an excessively long time delay, is recommended to compensate for the CCD time delay. However, the classical Smith predictor is sensitive to plant parameter variations, which could deteriorate the stability of the control system. Thus, in order to make a robust Smith predictor, a cascaded dual closed-loop including a high bandwidth velocity inner loop is introduced to reduce the influence of plant parameter variations. The low sensitivity to parameter variation of this method shows the significant improvement of the conventional Smith predictor control. Simultaneously, the analysis of tracking accuracy and the bandwidth of the FSM system is also presented. A series of comparative experimental results demonstrate that the tracking performance of the FSM control system can be effectively improved by the proposed approach.

1. Introduction

The fast steering mirrors (FSMs) are widely applied in optical tracking control systems, such as for free space optical communication, adaptive optics, line-of-sight (LOS) stabilization, [1-4] etc. A charge-coupled device (CCD) is customarily utilized to detect the LOS of target source in the focal plane of an imaging lens or lens array and it provides the tracking error directly as the input of the system. High control bandwidth facilitates better closed loop performance. In other words, a good CCD-based closed loop can make a high tracking performance of the FSM system. However, limited sampling frequency and time delay are the major reasons to restrict the bandwidth. In general, there are three factors causing the time delay to the closed loop system: exposure time of the CCD, image processing time, and data transmit time [5]. The time delay cannot be reduced to zero, which results in an ineffectiveness of a high bandwidth.

To improve the closed-loop performance of the FSM, feed-forward control, especially velocity feed-forward, is introduced to improve the tracking precision [6-7]. But the CCD tracker cannot provide target velocity directly, which has to be obtained by other estimation means, such as Kalman filter [8]. The newly introduced estimation means bring their selves time delay into the system, which restrict the feed-forward ability. In recent years, acceleration feedback control is recommended to enhance the robust of the FSM system; however, it almost has little effect on the closed loop bandwidth but only the disturbance attenuation [9]. The Smith predictor, which is famous for its delay-free characteristic and suitable for regulating systems with an excessively long time delay, has been widely used in many systems [10-13]. The classical Smith predictor is so sensitive to plant parameter variations that a little parameter mismatch could deteriorates the stability of the control system [14]. Most previous researches have focused on modifying the control structure to improve robust of the Smith predictor as the compensating precision mostly depends on the model of the controlled plant [15-16].

In this paper, to further enhance the model insensitivity of Smith predictor, we proposed a new FSM time delay compensation method, which combines the modified Smith predictor with a high bandwidth velocity closed-loop constructed by fiber-optic gyroscope (FOG). The high bandwidth inner loop is used to provide a robust controlled plant for outer control loop and the modified Smith predictor is utilized to deal with the time delay of the CCD-based FSM control system. A detailed introduction to the dynamic control model of the FSM is presented in Section 2. Section 3 and 4 introduces the theory analysis and the controller design. Section 5 sets up experiments to verify this method. Concluding remarks are presented in Section 6.

2. FSM System Control Model

A FSM is usually defined as a mirror mounted to a flexure support system and driven by actuators [17-18]. The configuration of the FSM control system of this research is illustrated in Figure 1. The controller is applied to implement the control algorithm. The driver actuates the voice coil motors to achieve target tracking of the FSM.

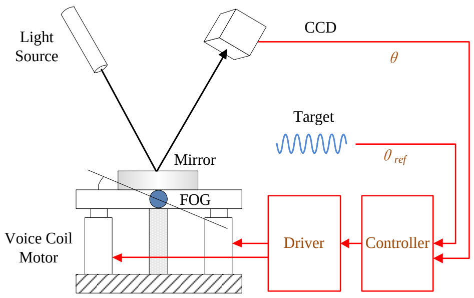

Figure 1. Configuration of the FSM control system

The mechanical part of the FSM is a typical resonance element and the voice coil motors is a typical first-order inertial element in the transfer model. Therefore, the FSM position open loop response can be expressed as follows [9, 17].

$$G_p(s) = \frac{\theta(s)}{U(s)} = \frac{K}{\dfrac{s^2}{\varpi_n^{\,2}} + \dfrac{2\xi}{\varpi_n}s + 1} \cdot \frac{1}{T_e s + 1} \tag{1}$$

The control strategy of FSM to compensate time delay goes into particulars as follows.

2.1 Classical Smith Predictor Control (SPC)

The classical Smith predictor control structure in FSM system is shown in Figure 2 [10].

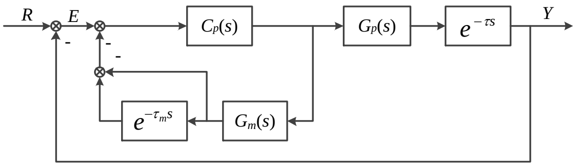

Figure 2. Classical Smith predictor control system

Where $G_p(s)$ is the controlled plant without pure time delay,

$C_p(s)$ is the position controller, $e^{-\tau s}$ is the time delay term which is mainly caused by CCD, $G_m(s)$ and τ_m are the models of the controlled plant $G_p(s)$ and τ .The controlled plant of SPC is expressed as:

$$P_{spc}(s) = G_p(s)e^{-\tau s} \qquad (2)$$

According to the control structure, the closed-loop transfer function of SPC is expressed as follows:

$$\begin{aligned} H_{spc}(\mathrm{s}) = \frac{Y(\mathrm{s})}{R(\mathrm{s})} &= \frac{\dfrac{C_p}{1+C_pG_m(1-e^{-\tau_m s})}\cdot P_{spc}}{1+\dfrac{C_p}{1+C_pG_m(1-e^{-\tau_m s})}\cdot P_{spc}} \\ &= \frac{C_pG_pe^{-\tau s}}{1+C_pG_m(1-e^{-\tau_m s})+C_pG_pe^{-\tau s}} \qquad (3) \\ &= \frac{C_pG_pe^{-\tau s}}{1+C_pG_m-C_pG_me^{-\tau_m s}+C_pG_pe^{-\tau s}} \end{aligned}$$

When a perfect matching between the models and the true transfer functions is assumed that is $G_m(s) = G_p(s)$ and $\tau_m = \tau$, Equation (3) is reduced to the following one:

$$H_{spc}(\mathrm{s}) = \frac{Y(\mathrm{s})}{R(\mathrm{s})} = \frac{C_pG_p}{1+C_pG_p}e^{-\tau s} \qquad (4)$$

As shown in Equation (4), the closed-loop characteristic equation does not contain the time delay term $e^{-\tau s}$. Thus, it could eliminate the influence of the stability of the FSM system, to improve the control performance. However, due to the sensor noise and circumstance changes, the deviation between the models and plant can be hardly reduced, which restricts the application of SPC in FSM system [14]. Therefore, a velocity inner loop can be considered to improve the performance of SPC.

2.2 Smith Predictor Control with Velocity Inner Loop (SPC-VIL)

The control structure of the improved SPC-VIL is shown in Figure 3.

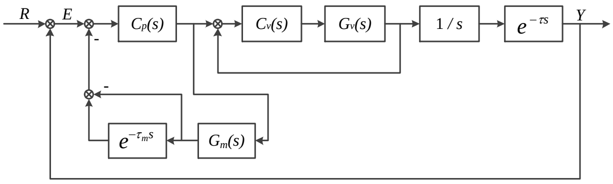

Figure 3. Smith predictor control with velocity inner loop

The FSM velocity open loop response $G_v(s)$ has a differential compare with $G_p(s)$, which is depicted in Equation (1).

$$G_v(s) = \frac{\dot{\theta}(s)}{U(s)} = \frac{K}{\dfrac{s^2}{\varpi_n{}^2}+\dfrac{2\xi}{\varpi_n}s+1}\cdot\frac{s}{T_es+1} \qquad (5)$$

According to the control structure, it is easy to get the closed-loop transfer function of velocity inner loop:

$$G_{v\_close}(s) = \frac{C_v G_v}{1 + C_v G_v} \qquad (6)$$

Where $C_v(s)$ is the velocity controller. Substituting $\frac{1}{s} \cdot G_{v\_close}(\mathrm{s})$ as the controlled plant $G_p(s)$ in SPC, consequently, the controlled plant of SPC-VIL could be expressed as:

$$P_{spc\_vil}(s) = \frac{1}{s} \cdot G_{v\_close}(s) \cdot e^{-\tau s} = \frac{1}{s} \cdot \frac{C_v G_v}{1 + C_v G_v} \cdot e^{-\tau s} \qquad (7)$$

Then, the closed-loop transfer function of SPC-VIL can be given:

$$H_{spc\_vil}(\mathrm{s}) = \frac{C_p \cdot \frac{1}{s} \cdot G_{v\_close}(s) \cdot e^{-\tau s}}{1 + C_p G_m (1 - e^{-\tau_m s}) + C_p \cdot \frac{1}{s} \cdot G_{v\_close}(s) \cdot e^{-\tau s}} \qquad (8)$$

Where G_m is the model of the transfer function $\frac{1}{s} \cdot G_{v\_close}(\mathrm{s})$. When a complete matching between the models and the controlled plant is assumed that is $G_m(s) = \frac{1}{s} \cdot G_{v\_close}(\mathrm{s})$ and $\tau_m = \tau$, Equation (8) can be simplified as follows:

$$H_{spc\_vil}(\mathrm{s}) = \frac{Y(\mathrm{s})}{R(\mathrm{s})} = \frac{C_p \cdot \frac{1}{s} \cdot G_{v\_close}(s)}{1 + C_p \cdot \frac{1}{s} \cdot G_{v\_close}(s)} \cdot e^{-\tau s} \qquad (9)$$

The improvement of SPC-VIL will be analyzed in Section 3.

3. Performance Analysis

As mentioned in Section 1, the Smith predictor is so sensitive to plant parameter variations that the presence of slight differences could affects the stability of the control system. Therefore, the improved robustness of controlled plant can enhance the performance of the Smith predictor. Ordinarily, the robustness of controlled plant is described by the sensitivity function, which is defined by Horowitz [19], and the expression of the sensitivity function is that the change of k leads to the change of $\varphi(s)$:

$$S_k^{\varphi} = \frac{d\varphi(s) / \varphi(s)}{dk / k} \qquad (10)$$

Substituting Equation (2) into Equation (10), the sensitivity function of SPC becomes:

$$\begin{aligned} S_{G_p}^{P_{spc}} &= \frac{\Delta P_{spc}(\mathrm{s}) / P_{spc}(\mathrm{s})}{\Delta G_p(\mathrm{s}) / G_p(\mathrm{s})} = \frac{(P_{spc}(\mathrm{s}) - P'_{spc}(\mathrm{s})) / P_{spc}(\mathrm{s})}{(G_p(\mathrm{s}) - G'_p(\mathrm{s})) / G_p(\mathrm{s})} \\ &= \frac{(G_p(\mathrm{s}) e^{-\tau s} - G'_p(\mathrm{s}) e^{-\tau s}) / G_p(\mathrm{s}) e^{-\tau s}}{(G_p(\mathrm{s}) - G'_p(\mathrm{s})) / G_p(\mathrm{s})} \\ &= 1 \end{aligned} \qquad (11)$$

Similarly, substituting Equation (7) into Equation (10), the sensitivity function of SPC-VIL becomes:

$$\begin{aligned} S_{G_v}^{P_{spc\_vil}} &= \frac{\Delta P_{spc\_vil}(\mathrm{s}) / P_{spc\_vil}(\mathrm{s})}{\Delta G_v(\mathrm{s}) / G_v(\mathrm{s})} \\ &= \frac{(P_{spc\_vil}(\mathrm{s}) - P'_{spc\_vil}(\mathrm{s}) / P_{spc\_vil}(\mathrm{s})}{(G_v(\mathrm{s}) - G'_v(\mathrm{s})) / G_v(\mathrm{s})} \\ &= \frac{1}{1 + C_v G'_v} \cdot \frac{C_v G_v - C_v G'_v}{C_v G_v} \cdot \frac{G_v}{G_v - G'_v} \\ &= \frac{1}{1 + C_v G'_v} \end{aligned} \tag{12}$$

Provided that the gain of the velocity controller is large enough, $S_{G_v}^{P_{spc\_vil}}$ is far less than 1. When the parameters of the plant change greatly, the controlled plant of SPC will be affected directly, and the stability of the FSM system will be further influenced. However, the controlled plant of SPC-VIL will not be affected. Actually, the gain of the velocity controller exceeds 300; therefore, the SPC-VIL is much more robust than the SPC.

4. Controller Design

4.1 Design of the inner loop controller

The FSM velocity open loop response measured by spectral analyzer is shown in Figure 4:

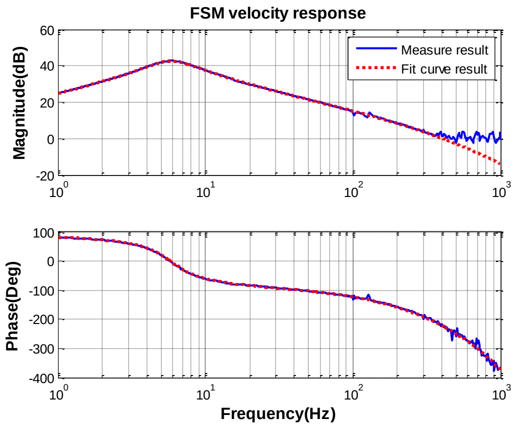

Figure 4. The FSM velocity open loop response

The mathematic transfer function model of the FSM velocity response can be obtained through the curve fitting method:

$$G(s) = \frac{2.7}{0.00073s^2 + 0.02s + 1} \cdot \frac{s}{0.0004s + 1} \tag{13}$$

The open loop natural frequency of FSM system ϖ_n is about 5.89Hz, and the damping factor ξ is about 0.37. Because of the differential and the second-order mechanical resonance in the FSM velocity response, the controller must have an integrator and a complete pole-zero cancellation to compensate them for total bandwidth stabilization when the system is closed. In order to increase the system gain, an integrator should be added. The velocity controller can be designed as follows:

$$C_v(\mathrm{s}) = 310.9 \cdot \frac{1}{s^2} \cdot \frac{0.00073s^2 + 0.02s + 1}{1} \cdot \frac{0.00079s + 1}{0.00036s + 1} \tag{14}$$

Where $0.00079s + 1$ is used to compensate phase loss, and $0.00036s + 1$ is used to filter the high-frequency noise.

4.2 Design of the model of plant

According to the previous analysis, the model of plant G_m should be designed as the transfer function $\frac{1}{s}\cdot G_{v\_close}(\mathrm{s})$. Substituting Equation (13) and Equation (14) into Equation (7), the transfer function of model G_m is:

$$\begin{aligned} G_m &= \frac{1}{s}\cdot G_{v\_close}(\mathrm{s}) \\ &= \frac{1}{s}\cdot\frac{\frac{310.9\cdot 2.7}{s}\cdot\frac{0.00079s+1}{0.00036s+1}\cdot\frac{1}{0.0004s+1}}{1+\frac{310.9\cdot 2.7}{s}\cdot\frac{0.00079s+1}{0.00036s+1}\cdot\frac{1}{0.0004s+1}} \\ &\approx \frac{1}{0.0012s^2+s} \\ &\approx \frac{1}{s} \end{aligned} \quad (15)$$

Because of the low CCD sampling rate which is 50 Hz in our experiments, the closed-loop transfer function of velocity loop can be simplified as an integrator at low frequency. The model G_m is designed as follows:

$$G_m = \frac{1.12}{s} \quad (16)$$

Where G_m is obtained from the position open-loop response of FSM when the velocity loop is closed. There is little difference in gain between measurement and theory.

4.3 Design of the outer loop controller

In the light of the control structure of SPC-VIL, it is clear that the controlled plant of outer loop is:

$$G_p(\mathrm{s}) = G_m - G_m e^{-\tau_m s} + \frac{1}{s}\cdot G_{\mathrm{v\_close}} e^{-\tau s} \quad (17)$$

Assumed a complete matching between the models and the true transfer functions, the controlled plant $G_p(\mathrm{s})$ can be simplified as follows:

$$G_p(\mathrm{s}) = G_m \quad (18)$$

The model G_m is designed as an integrator; therefore, the traditional PI controller can meet the position closed-loop control.

Because of the low CCD sampling rate and noise, the controlled plant is measured inaccurately at high frequency; actually, there is a mismatching between the models and the true controlled plant at above 10 Hz. Therefore, a lag element should be added to filter the mismatching. The outer loop controller is designed as:

$$C_p(s) = \frac{k_1 s + k_2}{s\cdot(T_1 s+1)} \quad (19)$$

Where k_1 and k_2 are the parameters of PI controller, the time constant T_1 is designed a little smaller than 0.02.

5 Experimental Verification

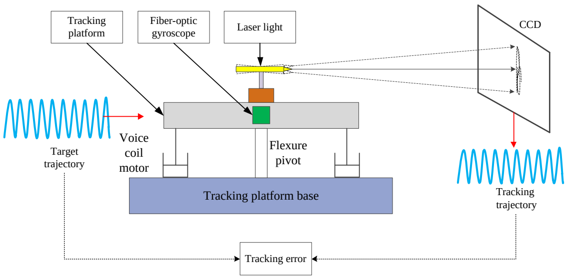

Figure 5. Principle of experimental apparatus

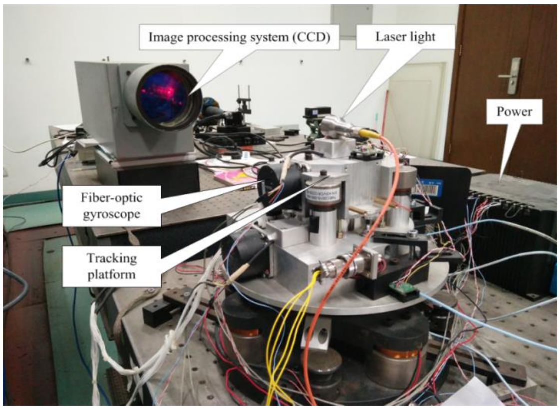

Figure 6. Prototype of experimental apparatus

The experimental setup is shown in Figure 5 and Figure 6, which includes a tracking platform, a fiber-optic gyroscope, a laser light, and an image processing system (CCD). The tracking platform is driven by the voice coil motors. The fiber-optic gyroscope is used to measure the tracking angular velocity of the platform, and the CCD is used to obtain the tracking trajectory. The program produces different frequency sine signals to simulate target trajectory, and the laser light shoots into the CCD when the FSM control system tracking the target. In the experiment, the fiber-optic gyroscope is at 5000Hz sampling frequency, and the CCD has only 50Hz working frequency with 40ms (2 frames) time delay.

According to the previous analysis, the Smith predictor can efficiently compensate the time-delay, which result in improving the phase in frequency domain. Therefore, the gain of position controller could be enhanced, which is significant for the tracking performance of the FSM control system.

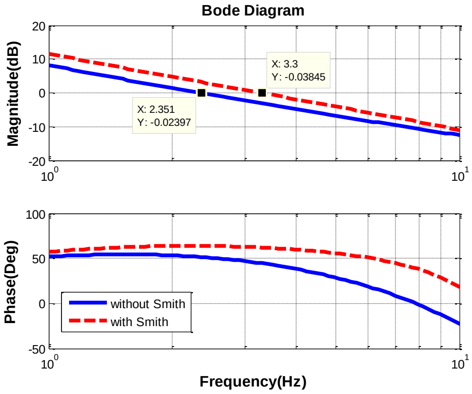

Figure 7. Position open loop response of the FSM system;

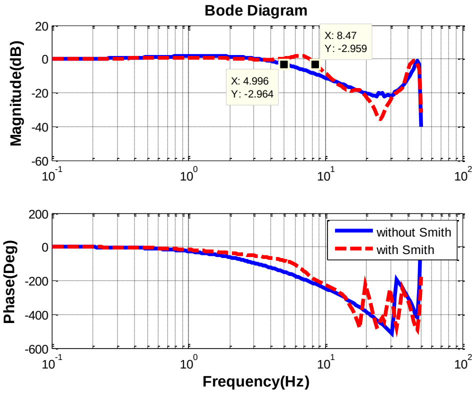

Figure 8. Position closed loop response of the FSM system;

As shown in Figure 7 and Figure 8 that with Smith predictor, the open loop cutoff frequency is improved from 2.351 Hz to 3.3 Hz and the closed loop bandwidth improved from 4.996 Hz to 8.47 Hz. The tracking error in different target frequency with and without Smith predictor is given in Figure 9 and Table 1:

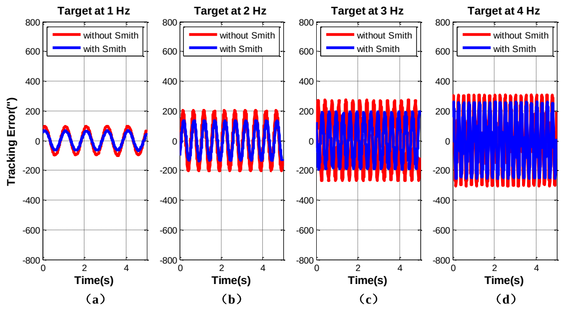

Figure 9. (a) the tracking error when target frequency at 1Hz; (b) the tracking error when target frequency at 2Hz; (c) the tracking error when target frequency at 3Hz; (d) the tracking error when target frequency at 4Hz.

Target frequency	**RMS[1](″)**		**PV[2](″)**	
	Without Smith	With Smith	Without Smith	With Smith
1 Hz	68.39	46.25	197.22	133.26
2 Hz	143.58	94.80	409.33	270.93
3 Hz	191.48	135.62	542.57	386.33
4 Hz	217.41	180.79	615.05	513.07

Table 1. The detailed circumstances of tracking error comparisons
[1] RMS stands for the Root Mean Square of the error.[2] PV stands for the Peak valley value of the error.

It is obvious that the tracking performance of the FSM control system with Smith predictor is improved at low frequency. However, the Smith predictor has a little effect at 4 Hz and almost is invalid at above 4 Hz. The reason is that the controlled plant is measured inaccurately at high frequency, and the mismatching between the models and the true controlled plant directly affects the ability of Smith predictor. The filter designed in Section 4 can reduce the mismatching partly. But, the improvement at low frequency is more significant to target tracking.

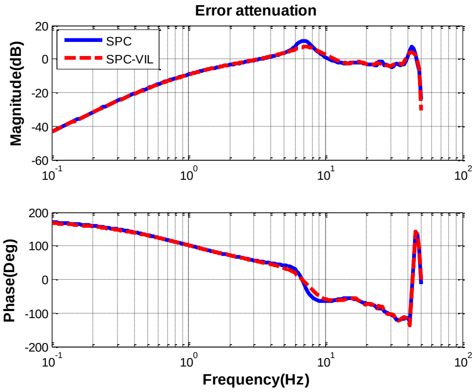

Figure 10. Error attenuation response

As discussed in Section 2, the ideal situation for Smith predictor is that the models completely match the controlled plant. When the position controller is designed as the inverse transfer function of controlled plant, it is easy to obtain the same closed loop transfer function between SPC and SPC-VIL that is $H_{spc}(s) = H_{spc\_vil}(s)$. In other words, the improvement of the tracking performance with Smith predictor has no difference between SPC and SPC-VIL when the models matching the controlled plant. Figure 10 shows the error attenuation response of SPC and SPC-VIL. The error attenuation of two kinds of control systems is almost equal at low frequency, and has a little difference at above 6 Hz.
However, the characteristics of the FSM system, particularly the gain of the FSM system, are changeable when suffering disturbance or in different circumstances [20]. As previous analyzed in Section 3, the SPC is more sensitive to plant parameter variations than SPC-VIL. The comparisons between SPC and SPC-VIL when the gain of the FSM system has changed are given below:

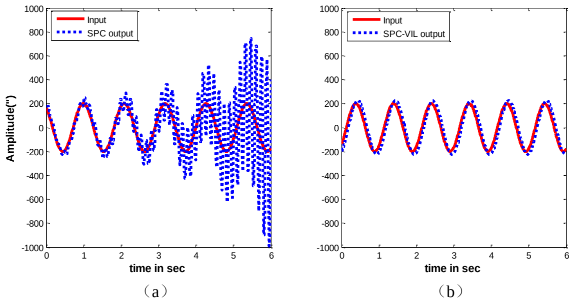

Figure 11. The outputs of FSM system (a) SPC; (b) SPC-VIL.

Figure 11 shows the FSM system outputs of SPC and SPC-VIL for sine input. It is obvious that the FSM system with SPC is unstable and the one with SPC-VIL is stable.

6 Conclusions

The Smith predictor was introduced to enhance the tracking performance of the FSM control system. However, the classical Smith predictor is sensitive to plant parameter variations. In this paper, a cascaded dual closed-loop including a high bandwidth velocity inner loop is proposed to reduce the influence of plant parameter variations. The sensitivity function shows that SPC-VIL can effectively enhance the robustness of the closed-loop control system, and the experimental results showed that the tracking performance of the FSM control system can be effectively improved by the proposed method.
Future work will concentrate on further improving the robustness of the closed-loop control system. The use of accelerometers may be an effective method to restrain the plant parameter variations, which will be our next work.

Acknowledgements
The authors sincerely thank the anonymous reviewers for their valuable comments and suggestions on this paper.

References

[1] R. W. Cochran and R. H. Vassar, 1990. “Fast steering mirrors in optical control systems,” *in Advances in Optical Structure Systems, Proc. SPIE* **1303**, 245–251.
[2] W. Liu, K. N. Yao, D. N. Huang, X. D. Lin, L. Wang and Y. W. Lv, 2016. "Performance evaluation of coherent free space optical communications with a double-stage fast-steering-mirror adaptive optics system depending on the Greenwood frequency," *Optics Express* **24(12)**, 13288-13302.
[3] J. Zhang, Q. Yang, K. Saito, K. Nozato, D. R. Williams and E. A. Rossi, 2015. "An adaptive optics imaging system designed for clinical use," *Biomedical Optics Express* **6(6)**, 2120-2137.
[4] J. M. Hilkert, 2009. “Development of mirror stabilization line-of-sight rate equations for an un-conventional sensor-to-gimbal orientation,” *Proc. SPIE* **7338**, 733803.
[5] A. A. Portillo, G. G. Ortiz, and C. Racho, 2001. “Fine pointing control for optical communications,” *in Proc. IEEE Aerospace Conf.,* Big Sky, MT, pp. 1541-1550.
[6] T. Tang, J. G. Ma, G. Ren and C. Y. Fu, 2010. "Compensating for some errors related to time delay in a charge-coupled-device-based fast steering mirror control system using a feedforward loop," *Optical Engineering* **49(7)**.
[7] T. Tang, J. Tian, D. J. Zhong and C. Y. Fu, 2016. "Combining Charge Couple Devices and Rate Sensors for the Feedforward Control System of a Charge Coupled Device Tracking Loop," *Sensors* **16(7)**.
[8] R. E. Kalman, 1960. “A new approach to linear filtering and prediction problems,” *Trans. ASME, J. Basic Eng. D* **82**, 35–45.
[9] J. Tian, W. S. Yang, Z. M. Peng, T. Tang and Z. J. Li, 2016. "Application of MEMS Accelerometers and Gyroscopes in Fast Steering Mirror Control Systems," *Sensors* **16(4)**.
[10] O.J.M. Smith, 1957. “Closer control of loops with dead time”, *Chemical Engineering Progress,* **53(5)**: 217-219.
[11] A. Salehiomran, R. Modirnia, B. Boulet and M. Rochette, 2014. "Optical Parametric Oscillator Longitudinal Modes Suppression Based on Smith Predictor Control Scheme," *Ieee Transactions on Control Systems Technology* **22(5)**, 2064-2072.
[12] C. K. Qi, F. Gao, X. C. Zhao, A. Y. Ren, Q. Wang, Q. Sun, Y. Hu and L. Qiao, 2016. "Smith predictor based delay compensation for a hardware-in-the-loop docking simulator," *Mechatronics* **36** 63-76.
[13] K. K. Tan, K. Y. Chua, S. Zhao, S. Yang and M. T. Tham, 2009. "Repetitive control approach towards automatic tuning of Smith predictor controllers," *Isa Transactions* **48(1)**, 16-23.
[14] Z. Palmor, 1980. "Stability properties of Smith dead-time compensator controllers," *International Journal of Control* **32(6),** 937-949.
[15] M. R. Matausek and A. I. Ribic, 2012. "Control of stable, integrating and unstable processes by the Modified Smith Predictor," *Journal of Process Control* **22(1)**, 338-343.
[16] D. G. Padhan and S. Majhi, 2012. "Modified Smith predictor based cascade control of unstable time delay processes," *Isa Transactions* **51(1)**, 95-104.
[17] Y.F. Lu, D.P. Fan, Z.Y. Zhang, 2013. “Theoretical and experimental determination of bandwidth for a two-axis fast steering mirror,” *Optik*, **124**, 2443-2449.
[18] X. Wu, S. H. Chen, B. Y. Shi, W. Chen and X. G. Xiong, 2011. "High-powered voice coil actuator for fast steering mirror," *Optical Engineering* **50(2)**.
[19] I.M. Horowitz, 1963. Synthesis of feedback systems, *Academic Press*, New York.
[20] Y. Mao, C. Deng, X. Gan and J. Tian, 2015. "The Effect of Physical Parameters of Inertial Stabilization Platform on Disturbance Rejection Ability and Its Improvement Method," in *Aopc 2015: Optical Design and Manufacturing Technologies* L. Li, K. P. Thompson and L. Zheng, Eds.